JOURNAL OF GUIDANCE, CONTROL, AND DYNAMICS
Vol. 30, No. 6, November–December 2007

Engineering Notes

ENGINEERING NOTES are short manuscripts describing new developments or important results of a preliminary nature. These Notes should not exceed 2500 words (where a figure or table counts as 200 words). Following informal review by the Editors, they may be published within a few months of the date of receipt. Style requirements are the same as for regular contributions (see inside back cover).

Space Vehicle Conflict Probability for Ellipsoidal Conflict Volumes

Russell P. Patera*
The Aerospace Corporation,
Los Angeles, California 90009-2957

DOI: 10.2514/1.30504

Introduction

SPACE vehicles can be protected against collisions with tracked space objects by executing collision avoidance maneuvers [1]. Once a space object is identified as a collision risk, plans can be made to maneuver the space vehicle to increase the closest approach distance to a safe level. In some cases, a maneuver is also needed to move the spacecraft back into its operational location. The key challenge in this process is identifying those conjunctions that pose the most collision risk.

Initially, the metric used to quantify collision risk was the predicted closest approach distance itself. Analysts recognized that the predicted closest approach distance is based on the nominal state vectors and does not include position uncertainty. To improve this situation, position error probability density ellipsoids were calculated based on the position error covariances of the respective space objects. Placing the ellipsoids on the nominal locations of the two objects at the time of conjunction enables one to determine the degree of overlap and hence collision risk. This "touching or overlapping ellipsoid" method can be used to identify risky conjunctions [2]. The next improvement was to actually compute the collision probability based on the nominal positions, position error covariances, and sizes of space objects. Although a significant amount of work has been done in deriving effective methods to compute collision probability [3–6], its effectiveness in identifying risky conjunctions is limited due to uncertainty in the size of the space objects, as well as the large position error uncertainties.

Recently, this author proposed using conflict probability to improve the situation [7]. Conflict probability is the probability that a conflict volume, which is centered on one object, will be penetrated by a secondary object. The aviation community uses cylindrical conflict volumes to identify potential midair collisions [8].

A spherically shaped conflict volume was found effective in identifying high-risk conjunctions [7]. However, the best shape for a conflict volume may not be spherical. Operators of the Earth-observing satellites use ellipsoidal-shaped keep-out regions to identify conjunctions requiring further analysis [9]. Therefore, conflict probability for ellipsoidal-shaped conflict volumes may be of value in detecting higher-risk conjunctions.

This Note presents a method to compute conflict probability for ellipsoidal-shaped conflict volumes. The approach of the current method is to transform the problem to the conflict volume frame, which has its coordinate axes aligned with the ellipsoid principal axes. A scale change is performed along two of the three axes such that all three axes are equal. This scale change symmetrizes the conflict volume, thereby transforming its shape from ellipsoidal to spherical. The combined position error covariance is transformed to the conflict volume frame and modified to account for the scale changes. Likewise, the positions and velocities of the space objects are transformed to the conflict volume frame and adjusted based on the scale changes. Once completed, the problem is reduced to one involving a spherical conflict volume. Because collision probability tools are already developed for spherical hardbodies, these tools can be used for conflict probability involving spherical conflict volumes. The relative motion can be linear or nonlinear, because methods have been developed for both cases [10].

A computer program was created to implement the method. The method was tested by comparing results with known solutions obtained using a completely different method [11]. Once validated, the computer tool was used to determine how well ellipsoidal conflict volumes can identify high-risk conjunctions.

A method was devised to determine the effectiveness of identifying risky conjunctions using three known space collision events [12,13]. The 23 December 1991 collision between object numbers 13,475 and 18,985; the 24 July 1996 collision between object numbers 18,208 and 23,606; and the 17 January 2005 collision between objects 7219 and 26,207 were investigated. Each collision event involved objects from unrelated launches. The entire unclassified catalog of tracked space objects was screened for conjunctions of less than 5 km over a five-day period centered at the time of each collision. Databases of space object sizes and estimated covariances were used in the calculations. The database was processed to produce collision and conflict probabilities. One would like the conflict probability associated with the actual collision event to rank highest among all conjunctions processed. The relative ranking of the actual collision event is a measure of the utility of a given parameter. The axes of the ellipsoidal conflict volume were varied in an attempt to find the most suitable shape. Results of the study are presented.

Analysis

The conflict probability for a spherical conflict volume is evaluated exactly the same as collision probability, except that the larger conflict volume replaces the spherical hardbody volume. Thus, new computations are not required. However, the conflict probability for an ellipsoidal conflict volume requires additional processing to account for the elliptical shape. The approach used here is to symmetrize the conflict volume. Once this is achieved, the calculation proceeds exactly the same as in the spherical conflict probability case.

The conflict volume is centered on the secondary space object. The orientation of the axes of the conflict volume ellipsoid is determined by the analyst. Because most conjunctions involve space vehicles with small orbital eccentricities, the local horizontal or spacecraft coordinate frame was thought to be most appropriate. Thus, the axes of the conflict volume ellipsoid are aligned with the axes of the local

Received 16 February 2007; revision received 21 June 2007; accepted for publication 27 June 2007.

*Ph.D., Senior Engineering Specialist, Center for Orbital and Reentry Debris Studies, Mail Stop M4-066.

horizontal frame. The position and velocity vectors are used to establish the axes of the local frame.

$$\mathbf{Y}_l = \frac{\mathbf{v} \times \mathbf{r}}{|\mathbf{v}||\mathbf{r}|} \tag{1}$$

$$\mathbf{Z}_l = \frac{-\mathbf{r}}{|\mathbf{r}|} \tag{2}$$

$$\mathbf{X}_l = \mathbf{Y}_l \times \mathbf{Z}_l \tag{3}$$

The local-to-inertial transformation is given by

$$U = (\mathbf{X}_l \;\; \mathbf{Y}_l \;\; \mathbf{Z}_l) \tag{4}$$

If a different orientation of the conflict volume ellipsoid was selected, the definition of U would change but the analysis that follows would remain the same.

Let the equation defining the ellipsoidal conflict volume be given by

$$\frac{x_l^2}{a^2} + \frac{y_l^2}{b^2} + \frac{z_l^2}{c^2} = 1 \tag{5}$$

where the axes of the ellipsoid are aligned with the axes of the local frame.

Scale changes are applied along the $\mathbf{Y}_l$ and $\mathbf{Z}_l$ axes, given by

$$y_l' = y_l\left(\frac{a}{b}\right) \tag{6}$$

$$z_l' = z_l\left(\frac{a}{c}\right) \tag{7}$$

Using Eqs. (6) and (7) in Eq. (5) transforms the ellipsoid to a sphere of radius a.

$$x_l'^2 + y_l'^2 + z_l'^2 = a^2 \tag{8}$$

In this manner, the scale change transforms the elliptical conflict volume to a spherical conflict volume.

The positions and velocities for both primary and secondary objects are transformed to the local frame and scaled to be consistent with the scaled conflict volume. Because U is an orthogonal transformation, its inverse is simply the transpose and one finds

$$\mathbf{r}_l = U^T\mathbf{r} \tag{9}$$

$$\mathbf{v}_l = U^T\mathbf{v} \tag{10}$$

Define the scale matrix as

$$S = \begin{pmatrix} 1 & 0 & 0 \\ 0 & a/b & 0 \\ 0 & 0 & a/c \end{pmatrix} \tag{11}$$

The positions and velocities are scaled according to S.

$$\mathbf{r}'_l = S\mathbf{r}_l \tag{12}$$

$$\mathbf{v}'_l = S\mathbf{v}_l \tag{13}$$

The combined covariance matrix in the inertial frame, $\mathbf{C}$, is transformed to the local or conflict ellipsoid frame by the following transformation:

$$\mathbf{C}_l = U^T\mathbf{C}U \tag{14}$$

The covariance matrix in the local frame is transformed by the scale change as

$$\mathbf{C}'_l = S\mathbf{C}_l S^T \tag{15}$$

The conflict probability calculation is now performed using the methods developed for collision probability prediction. This can be done because the scale change transformed the elliptical conflict volume to a spherical conflict volume, and the positions, velocities, and combined covariance matrix were changed accordingly.

Numerical Testing

Several numerical tests were defined to check the validity of the proposed method. The test case has positions and velocities given by

$$\mathbf{r}_1 = \begin{pmatrix} 1 \\ 0 \\ 0 \end{pmatrix} \text{km} \tag{16}$$

$$\mathbf{v}_1 = \begin{pmatrix} 0 \\ 1 \\ 0 \end{pmatrix} \text{km/s} \tag{17}$$

$$\mathbf{r}_2 = \begin{pmatrix} 19 \\ 0 \\ 0 \end{pmatrix} \text{km} \tag{18}$$

$$\mathbf{v}_2 = \begin{pmatrix} 0 \\ -1 \\ 0 \end{pmatrix} \text{km/s} \tag{19}$$

The encounter plane is perpendicular to the relative velocity vector. The x axis of the encounter plane is directed from the primary object to the secondary object, as illustrated in Fig. 1. The combined position error ellipsoid is centered on the primary object and the ellipsoidal conflict volume is centered on the secondary object. The maximum and minimum standard deviations are 12 and 2 km, respectively. The angle between the maximum standard deviation axis and the x axis, a, was varied, as shown in Fig. 1. Several values of conflict volume eccentricity were selected for the set of test cases examined. The associated values of a, b, and c, which define the conflict volume in three dimensions via Eq. (5), are included in Table 1 with other parameters defining the set of test cases.

The conflict probability is just the integral of the position error probability density over the conflict area in the encounter plane. As presented in previous work, the two-dimensional area integral is reduced to a one-dimensional definite integral about the perimeter of

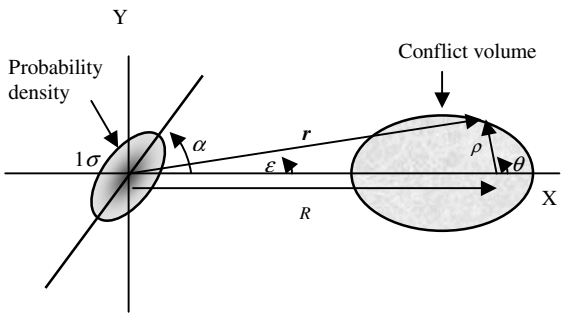

Fig. 1 Elliptical conflict volume in the encounter frame before symmetrization.

Table 1 Conflict probability test-case results

ρ_0	0.03 km	0.03 km	0.03 km	0.6 km	0.6 km	0.6 km
Eccentricity	0	0.5	0.9	0	0.5	0.9
A	variable	variable	variable	variable	variable	variable
B	0.03 km	0.0346 km	0.0688 km	0.6 km	0.6929 km	1.3765 km
C	0.03 km	0.04 km	0.1579 km	0.6 km	0.8 km	3.1579 km
$P(\alpha = 0)$	6.087e − 6	9.3716e − 6	7.349e − 5	2.4088e − 3	3.6959e − 3	2.8059e − 2
$P(\alpha = 90)$	4.842e − 23	7.4682e − 23	6.204e − 22	4.238e − 20	1.0806e − 19	1.8566e − 15
$P(\alpha = 26.56)$	2.3207e − 9	3.5737e − 9	2.814e − 8	1.0934e − 6	1.8033e − 6	4.2959e − 5

the conflict area [11]. This is achieved by symmetrizing the position error probability density, as illustrated in Fig. 2.

Thus, the probability calculation is reduced to a simple one-dimensional integral (Eq. 8 in [11]) given by [11]

$$P = \frac{f}{2\pi}\int_0^{2\pi}\left(\frac{\rho^2 + R\rho\cos(\theta) + R(\mathrm{d}\rho/\mathrm{d}\theta)\sin(\theta)}{r'^2}\right) \times \left[1 - \exp\left(\frac{-r'^2}{2\sigma^2}\right)\right]\mathrm{d}\theta \tag{20}$$

where f is the ratio of the maximum to minimum standard deviation of the position probability density ellipse in Fig. 1, and R, α, θ, and ρ are defined in Fig. 1.

$$r'^2 = [R + \rho\cos(\theta)]^2[\cos^2(\alpha) + f^2\sin^2(\alpha)] + \rho^2\sin^2(\theta)\,[\sin^2(\alpha) + f^2\cos^2(\alpha)] + 2\rho(1 - f^2)\cos(\alpha)\sin(\alpha)\sin(\theta)[R + \rho\cos(\theta)] \tag{21}$$

Details of the derivation of Eqs. (20) and (21) can be found in the original work [11]. Notice that r' is a function of θ, and ρ may be a function of θ if the conflict area is not circular. The definition of the elliptical conflict volume in the encounter plane is given by

$$\rho(\theta) = \frac{\rho_0}{1 + e\cos(\theta)} \tag{22}$$

where ρ_0 is the semilatus rectum of the ellipse.

This polar equation defining the ellipse was chosen because it is ideally suited for use in Eq. (20).

The derivative of ρ is used in Eq. (20) and is given by

$$\frac{\mathrm{d}\rho}{\mathrm{d}\theta} = \frac{e\rho_0\sin(\theta)}{[1 + e\cos(\theta)]^2} \tag{23}$$

Further details of implementing Eq. (20) can be found in the original work [11].

The conflict probability values in Table 1 were computed using Eq. (20) and the current proposed method. The ellipsoidal parameters a, b, and c defined the conflict volume, which was centered on the secondary object. The respective transformations to the local frame of the secondary object and scale changes were executed. The transformed parameters were then processed using standard techniques, because the new conflict volume was spherical. The resulting conflict probabilities were exactly the same as those computed earlier using Eq. (20). The agreement between the two methods serves to validate the new proposed method.

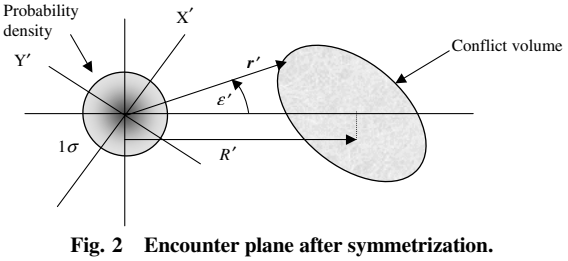

Fig. 2 Encounter plane after symmetrization.

Table 2 Covariance definitions for orbit types

Terms	LEO	MEO	HEO	GEO
X, km	1.5	5.27	13.27	10.6
Y, km	0.42	3.48	8.31	6.9
Z, km	0.23	1.43	3.68	2.91
$\mathrm{D}x/\mathrm{d}t$, km/day	0.28	0.14	0.93	0.72
$\mathrm{D}y/\mathrm{d}t$, km/day	0.04	0.01	0.07	0.14
$\mathrm{D}z/\mathrm{d}t$, km/day	0.04	0.02	0.10	0.09
$\mathrm{d}^2x/\mathrm{d}t^2$, km^2/day^2	0.07	0.01	0.22	0.13
$\mathrm{d}^2y/\mathrm{d}t^2$, km^2/day^2	0	0	0	0.01
$\mathrm{d}^2z/\mathrm{d}t^2$, km^2/day^2	0	0	0	0

Conjunction Risk Prediction

The ability of the conflict volume method to identify or predict high-risk conjunctions was evaluated with space object data. The actual risk of a particular conjunction is generally not known, and so there is no obvious way to evaluate a risk prediction parameter. However, when a collision occurs, one knows that the conjunction was extremely risky and a useful collision-risk parameter should indicate this very high risk. Therefore, data from three known space collision events were used to determine the effectiveness of conflict probability.

The 23 December 1991 collision between object numbers 13,475 and 18,985; the 24 July 1996 collision between object numbers 18,208 and 23,606; and the 17 January 2005 collision between objects 7219 and 268207 were investigated. The entire unclassified catalog of tracked space objects was screened for conjunctions of less than 5 km over a five-day period centered at the time of each collision. There were 7525, 8718, and 10,420 conjunctions for the 1991, 1996, and 2005 collision events, respectively. A database of covariance data was used for each conjunction event, based on the orbits of the respective space objects. Table 2 contains the covariance

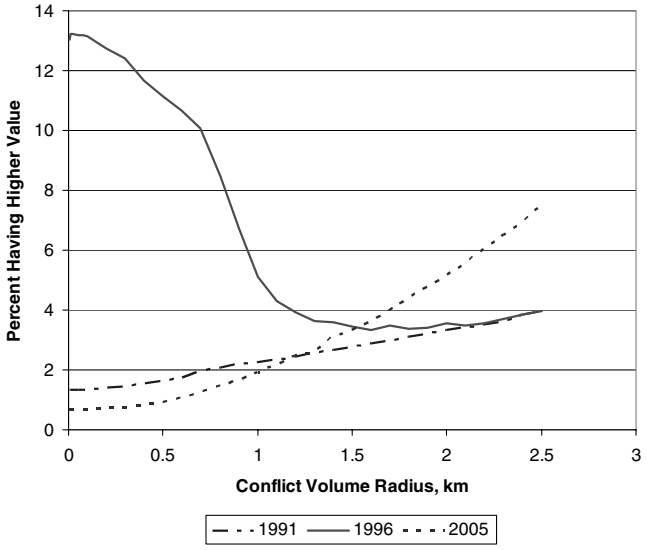

Fig. 3 Conflict probability performance versus conflict volume radius for three collision events; lower values signify better performance.

Table 3 Collision event summary

Event	Miss distance (km)/ percentile	Collision probability/ percentile	Maximum conjunction probability/percentile	Conflict probability (sphere)/ percentile	Conflict probability (pancake)/percentile
1991	0.814/92.173%	1.1×10^{-5}/91.083%	1.3×10^{-5}/87.535%	0.556/97.754%	0.433/98.525%
1996	1.129/91.340%	2.9×10^{-7}/87.910%	1.9×10^{-6}/78.149%	0.312/94.896%	0.090/88.278%
2005	0.107/99.827%	7.9×10^{-7}/94.731%	1.2×10^{-4}/99.011%	0.479/98.081%	0.400/99.060%

data with both linear and quadratic growth terms in the respective local coordinate frames of each space object.

The conflict probability was computed for each conjunction. The conjunctions were then arranged from lowest to highest value of conflict probability. The actual collision event is expected to have one of the highest conjunction probabilities. Thus, the percentage of conjunctions having lower conflict probability than the actual collision serves as a measure of effectiveness of conflict probability. The size and shape of the conflict ellipsoid were adjusted to increase the percentage of conjunctions having lower conflict probability. This serves to increase the ability of conflict probability to identify high-risk conjunctions.

Initially, a spherical conflict volume was used for each collision event. The size of the conflict volume was varied and the associated ranking of the conflict probability of the collision event with respect to the other conjunctions was computed. Figure 3 illustrates the percentage of conjunctions having higher conflict probability versus the radius of the spherical conflict volume. A smaller conflict volume radius performs better for the 1991 and 2005 events. Conflict volumes greater than 1 km performed better for the 1996 collision event.

Values of various conjunction risk parameters and associated percentile ranking of each collision event were placed in Table 3. Collision probability, nominal predicted miss distance, and conflict probability for a 1-km sphere were evaluated for each collision event. The "maximum conjunction probability" parameter [14], which is found by varying position error, was also evaluated and the results are presented in Table 3. A pancake-shaped ellipsoidal conflict volume with a radius of 1 km and a thickness in the radial direction of 500 m was also included in the analysis. This ellipsoid can be described by $a = 1$ km, $b = 1$ km, and $c = 500$ m. A football-shaped ellipsoid was also tried, but it gave results no better than a spherical conflict volume and so its results were not included in Table 3.

Table 3 indicates that nominal miss distance performs roughly the same as collision probability. Maximum conjunction probability does not perform as well, except for cases involving very small nominal miss distance, as in the 2005 event, which had a nominal miss of about 100 m. Conflict probability using a 1-km spherical conflict volume performs significantly better than the others. The ellipsoidal pancake volume performs even better than the spherical volume for the 1991 and 2005 events. However, it performs worse for the 1996 event. It appears that the 1996 event has peculiar behavior, because performance improves with increasing conflict volume size, as exhibited in Fig. 3.

Conclusions

The effectiveness of collision-risk metrics such as miss distance, collision probability, maximum conjunction probability, and conflict probability can be determined by analyzing real space collision events. The higher the percentile ranking of an actual collision event among the set of risky conjunction, the better the metric is at identifying collision risk. Analysis of three space collision events indicated that maximum conjunction probability is not as effective as other metrics are in identifying risky conjunctions. Conflict probability outperformed collision probability and miss distance. Ellipsoidal conflict volumes are better than simple spherical conflict volumes because the shape of the ellipsoid can be adjusted to improve results. In fact, a pancake-shaped conflict volume with a radius of 1 km and a thickness of 500 m was found superior to a 1-km spherical conflict volume. One reason for the improvement could be that the conflict volume shape is similar to the position error ellipsoid, in that the radial position uncertainty is smaller than the uncertainty associated with the other two axes. As more space collision events are uncovered, additional analyses should be performed to determine the conflict volume size and shape that is most effective in predicting hazardous conjunctions.

Acknowledgment

Thanks are extended to Vladimir Chobotov, Charles Gray, and James Paget for reviewing this document and providing valuable suggestions. The author greatly appreciates the work of Eric George in developing the statistical conjunction data for actual space collision events.

References

[1] Patera, R. P., and Peterson, G. E., "Space Vehicle Maneuver Method to Lower Collision Risk to an Acceptable Level," *Journal of Guidance, Control, and Dynamics*, Vol. 26, No. 2, 2003, pp. 233–237.

[2] Gist, R. G., and Oltrogge, D. L., "Collision Vision: Covariance Modeling and Intersection Detection for Spacecraft Situational Awareness," Astrodynamics Specialist Conference, Girdwood, AK, American Astronautical Society Paper AAS-351, Aug. 1999.

[3] Alfriend, K. T., Akella, M. R., Lee, D., Frisbee, J., and Foster, J. L., "Probability of Collision Error Analysis," *Space Debris*, Vol. 1, No. 1, 1999, pp. 21–35. doi:10.1023/A:1010056509803

[4] Berend, N., "Estimation of the Probability of Collision Between Two Catalogued Orbiting Objects," *Advances in Space Research*, Vol. 23, No. 1, 1999, pp. 243–247. doi:10.1016/S0273-1177(99)00009-5

[5] Chan, K., "Collision Probability Analysis for Earth Orbiting Satellites," *Advances in the Astronautical Sciences*, Vol. 96, Univelt, San Diego, CA, 1997, pp. 1033–1048.

[6] Patera, R. P., "General Method for Calculating Satellite Collision Probability," *Journal of Guidance, Control, and Dynamics*, Vol. 24, No. 4, 2001, pp. 716–722.

[7] Patera, R. P., "Space Vehicle Conflict Avoidance Analysis," *Journal of Guidance, Control, and Dynamics*, Vol. 30, No. 2, 2007, pp. 492–498. doi:10.2514/1.24067

[8] Paielli, R. A., Erzberger, H., "Conflict Probability Estimation for Free Flight," *Journal of Guidance, Control, and Dynamics*, Vol. 20, No. 3, 1997, pp. 588–596.

[9] Newman, L., Duncan, M., and McKinley, D., "Establishment and Implementation of a Close Approach Evaluation and Avoidance Process for Earth Observing System Missions," AIAA/AAS Astrodynamics Specialist Conference, Keystone, CO, AIAA Paper No. 2006-6291, Aug. 2006.

[10] Patera, R. P., "Collision Probability for Larger Bodies Having Non-Linear Relative Motion," *Journal of Guidance, Control, and Dynamics*, Vol. 29, No. 6, 2006, pp. 1468–1472. doi: 10.2514/1.23509also American Astronautical Society Paper 05-309, Aug. 2005.

[11] Patera, R. P., "Calculating Collision Probability for Arbitrary Space-Vehicle Shapes via Numerical Quadrature," *Journal of Guidance, Control, and Dynamics*, Vol. 28, No. 6, 2005, pp. 1326–1328.

[12] Alby, F., Lansard, E., and Michal, T., "Collision of Cerise with Space Debris," *Second European Conference on Space Debris*, ESA-SP 393, European Space Operations Center, Darmstadt, Germany, Mar. 1997, p. 589.

[13] "Accidental Collisions of Cataloged Satellites Identified," *The Orbital Debris Quarterly News*, Vol. 9, No. 2, 2005, pp. 1–2.

[14] Alfano, S., "Relating Position Uncertainty to Maximum Conjunction Probability," *Journal of the Astronautical Sciences*, Vol. 53, No. 2, 2005, pp. 193–205.